Voltammetric Studies of Dendrimer Multilayers: Layer-by-Layer Assembly of Metal-Peptide Dendrimers Multilayers

Francis E. Appoh,[1]* Heinz-Bernhard Kraatz[2]

[1]*Department of Chemistry, University of Saskatchewan, Saskatoon, Saskatchewan, Canada S7N 5C9*
[2]*Department of Chemistry, The University of Western Ontario, London, Ontario, Canada N6A 5B7*

Received 6 March 2008; accepted 27 June 2008
DOI 10.1002/app.28980
Published online 13 October 2008 in Wiley InterScience (www.interscience.wiley.com).

ABSTRACT: Multilayer films of metal-peptide dendrimers having a ferrocene core were constructed on gold surfaces functionalized with mercaptoundecanoic acid using a layer-by-layer approach for film construction. Cyclic voltammetry (CV) and differential pulse voltammetry (DPV) were used to monitor the redox activity and stability of these films. The multilayer films showed good stability and exhibited direct electron transfer with the underlying electrode. The specific active surface concentration can be varied by the number of layers, the nature of the dendrimer, and the nature of metal ions used. © 2008 Wiley Periodicals, Inc. J Appl Polym Sci 111: 709–723, 2009

Key words: multilayers; ferrocene; dendrimers; metal ions; cyclic voltammetry; differential pulse voltammetry

INTRODUCTION

The layer-by-layer (LbL) self-assembly technique for fabricating ultrathin films was pioneered by Iler[1] with rigid colloidal particles, and popularized by Decher exploiting the electrostatic attraction between cationic and anionic polyelectrolytes.[2,3] Because of the simplicity of this technique, it has been used for the preparation of a series of layered materials composed of conductive polymers,[4] proteins,[5,6] DNA,[7,8] dendrimers,[9–12] polysaccharides,[13] organic-metal complexes,[14–20] quantum dots,[21] nanoparticles,[22] exploiting electrostatic interactions, covalent bond formation, and hydrogen bonding interactions or the formation of metal complexes. For example, LbL films of poly(L-lysine) (PLL) and poly(L-glutamic acid) (PLGA) were prepared by carefully controlling the pH of the deposition solution, which regulates the film composition by controlling the charge density of the polypeptides.[23–25] Recently, Voegel and coworkers studied multilayer films constructed from PLL solution and a mixed solution containing PLGA and poly(L-aspartic acid), and demonstrated that the proportion of β-sheet content varied with the composition of the solution.[26] In LbL films containing alternate layers of PLL and poly(maleic acid-*co*-a-methylstyrene) (PMA-MS) or poly(vinyl sulfate) (PVS), the α-helicity of the peptide is maintained in the presence of $NaClO_4$.[27]

Cheng and Corn reported the fabrication of ultrathin polypeptide multilayers from PLGA and PLL at gold electrodes functionalized with 11-mercaptoundecanoic acid (MUA) and the incorporation of the $[Fe(CN)_6]^{3-/4-}$ redox couple.[28] In an electrostatically formed LbL assembly of PLL/carboxylic acid functionalized polyphenylene dendrimers and hybrid multilayers of L-lysine dendrimers and colloidal gold nanocrystals, Kim et al. characterized the permeability of the dendrimer layers by monitoring the electrochemical response in the presence of $[Fe(CN)_6]^{3-/4-}$.[29] In this system, the interfacial resistance, originating from the electrostatic repulsion of the negatively charged redox probe and the negatively charged interface, increases with the number of layers. Systems that have a redox mediator as an integral part of the multilayer were reported for ferrocene (Fc)-modified poly(amine)s,[30] Os-modified polymers,[31,32] and for biological redox proteins, such as *cyt c*.[33,34]

The use of dendrimers as molecular building blocks for LBL assemblies is of particular interest because their size, geometry, and chemical functionality can be controlled to obtain well-defined films. There are only a limited number of examples reported in which LbL are formed by exploiting the coordination of metal ions to dendrimers. Watanabe

Additional Supporting Information may be found in the online version of this article.

**Present address:* McMaster Institute of Applied Radiation Sciences, McMaster University, 1280 Main Street West, Hamilton, Ontario, Canada L8S 4K1.
Correspondence to: F. E. Appoh (appohfr@mcmaster.ca).
Contract grant sponsor: NSERC.

and Regen employed repetitive deposition of Pt^{2+} and PAMAM dendrimers to build multilayers.[35] De Schryver and coworkers assembled multilayers of carboxylic acid terminal polyphenylene dendrimers on MUA films exploiting the coordination to Cu^{2+} and showed by AFM that the strong interaction between the dendrimers and the Cu^{2+} ions led to a compression or deformation of the film and also resulted in a decreased height of the dendrimer.[36]

Amino acids are important low molecular weight ligands in biological systems. Aspartate (Asp) and glutamate (Glu) side chains are among the most common amino acid ligands that coordinate to cofactors in metalloproteins, where they play various roles. When incorporated into proteins the side chain carboxylate groups of the aspartyl and glutamyl residues constitute the metal binding sites, e.g. in various zinc enzymes such as carboxypeptidases A and B and alkaline phosphatase and in iron proteins such as hemerythrin. The EF-hand proteins (EF elongation factor), such as calmodulin and Troponin C, are known to contain Asp/Glu side chains which are selective for Ca(II) binding. Furthermore, the Glu residue in calmodulin binds to Ca(II) in a bidentate fashion and is known to lead to a series of reactions whereas the protein is not active when coordinated to Mg(II) thus, demonstrating the selectivity of the proteins.[37–39] The apparent similarities between Ca(II) and lanthanides, particularly with regards to ionic radii, ligand exchange rates, and coordination numbers, have justified their isomorphous replacement in biological macromolecules. For example, it has been shown that Tb(III) is able to displace Ca(II) in the calcuim binding sites of α- and β-crystallins (a protein responsible for opacity in eye lenses).[40] In addition, it has been reported that La^{3+} increases the activity of phosphodiesterase by competing with Ca^{2+} at low concentrations[41] and it has been shown that La^{3+} improves the capture of light energy of chlorophyll by replacing Mg^{2+}.[42] Poly-glutamic acid (PGA) and poly-L-aspartate have been evaluated as potential biosorbent material for use in the removal of heavy metals from aqueous solution. Recently, poly-L-aspartate was shown to complex metals like Eu^{3+}, Ce^{3+}, La^{3+}, Cu^{2+}, and Pb^{2+}, and to act as corrosion inhibitors for steel and iron, a property that has been ascribed to the carboxylate side chain of aspartic acid.[43,44] L-glutamic acid [$HOOC(CH_2)_2CH(NH_2)COOH$] is a mono amino dicarboxylic α-amino acid. Being a monoamino diacid, glutamic acid also offers a unique AB_2 architecture for the construction of dendrimers. However, the use of glutamic acid as a dendrimer constructs has received very little attention compared to the lysine-based dendrimers and metal complexes of their dendrimers is non-existent. Peptide dendrimers containing redox active moiety acts as artificial models for biomolecules and can be used to mimic biological processes. Multilayer films incorporated with these biological materials would therefore have potential applications in enzyme immobilizations and drug delivery.

We have recently reported the synthesized Fc based glutamic acid ester dendrimers and prepared their deposition on MUA functionalized monolayers on gold electrodes. Additionally, we have reported the synthesis of cystamine functionalized glutamic acid dendrimer analogues and demonstrated their deposition and interaction of metal cations Ca^{2+} and Tb^{3+} at the gold electrode interfaces.[45–47] The materials display strong intramolecular as well as intermolecular Hydrogen bonding with carboxylate interfaces and that the redox properties of the core are attenuated by the increase in the peptide dendritic sphere and metal ion interactions. In this study, we explore the use of these metal ions to assemble LbL films of peptide dendrimers. These metal ions prefer coordination to the carboxylic acid site over peptide backbone coordination,[47–49] and should be ideally suited for the controlled formation of LbL films involving peptide dendrimers. The choice of glutamic acid over aspartic acid is because the latter is pruned to cyclization during base hydrolysis, the method of choice in the preparation of the free acid terminal from the ester analogues. The glutamic acid-based dendrimer possesses a Fc core (a well-defined one-step redox moiety) allowing the quantification of the redox label by voltammetric methods and thereby of the Fc-dendrimer within each given layer.

EXPERIMENTAL

General procedure

All synthesis were carried out in air unless otherwise indicated. CH_2Cl_2 and $CHCl_3$ (BDH; ACS grade) used for synthesis, FT-IR and electrochemistry were dried (CaH_2), and distilled under N_2 prior to use. Acetone, MeOH, diethyl ether (BDH; ACS grade), hexanes (Fisher; HPLC grade), $CHCl_3$, and CH_2Cl_2 used for the purpose of purification were used as received. $CDCl_3$ and CD_3CN (Aldrich) were dried by, and stored over molecular sieves (8-12 mesh; 4 Å effective pore size; Fisher) before use. EDC, HOBt, H-Glu-OEt·HCl (Aldrich), Na_2SO_4, $NaHCO_3$ (VWR), and FcCOOH (Strem) were used as received. Et_3N (BDH; ACS grade) used in Fc-amino acid couplings was dried by molecular sieves when used in stoichiometric quantities. For column chromatography, a column with a width of 2.7 cm (ID) and a length of 45 cm was packed 18–22 cm high with 230–400 mesh silica gel (VWR). For TLC, aluminum plates coated with silica gel 60 F_{254} (EM

Science) were used. NMR spectra were recorded on either a Bruker AMX-300 spectrometer operating at 300.135 MHz (^{1}H) and 75.478 MHz (^{13}C{^{1}H}), or on a Bruker AMX-500 spectrometer operating at 500 MHz (^{1}H) and 125 MHz (^{13}C{^{1}H}). Peak positions in both ^{1}H and ^{13}C spectra are reported in ppm relative to TMS. ^{1}H NMR spectra of Fc-peptides are referenced to the $DMSO_{d6}$ resonance (δ 2.50 ppm) of an external standard ($CDCl_3/CH_2Cl_2$). All ^{13}C{^{1}H} spectra are referenced to the $CDCl_3$ signal at δ 77.23 ppm. The synthesis of glutamic-acid dendrimer esters (**G1OEt–G5OEt**) was carried out according to the literature procedure.[46] Scheme 1 shows the sketch of the synthesis of carboxylate terminal dendrimer G4OH from its G4OEt analogue and position of the Fc moiety with respect to the general dendrimer architecture.

Preparation and characterization of G1OH

Compound **G1OEt** (1.1 g, 3.0 m*M*) was dissolved in 40 mL MeOH and NaOH (100 mg, 2.4 m*M*) was added and the reaction mixture was stirred at room temperature for 3 h. The disappearance of the starting material was followed by TLC. The HCl (1*N*) was added to neutralize the solution. The solvent was removed and the residue was purified by column chromatography (R_f = 0.32 AcOH/MeOH/$CHCl_3$ 1 : 2 : 17) giving an orange solid. Similar procedure was used for the preparation of **G2OH** to **G5OH.**

Yield: 0.62 g, 77%. FAB-MS: m/e calculated for $C_{16}H_{17}NO_5Fe$ = 360.0534 $[M+1]^+$, found: 360.0766. ^{1}H NMR (δ in ppm, DMSO-d_6): 12.40 (2H, m, OH), 7.84 (1H, d, J = 8.0 Hz , NH), 4.02 (1H, m, CH^{α}-Glu), 4.87 (1H, s, H^o Cp), 4.82 (1H, s, H^o Cp), 4.43 (4H, s, H^m Cp), 4.21 (5H, s, Cp), 2.30 (2H, m, CH_2^{γ}-Glu), 2.16 (1H, m, CH_2^{β}-Glu), 1.97 (1H, m, CH_2^{β}-Glu). ^{13}C NMR (δ in ppm, DMSO-d_6): 174.7, 174.5, 170.7 (C-carbonyl), 76.7 (quaternary C-substituted Cp), 70.9 (C^o-Cp), 70.2 (C-unsubstituted Cp), 69.2 (C^m-Cp), 52.1 (CH^{α}-Glu), 31.2 (CH_2^{β}-Glu), 26.7 (CH_2^{γ}-Glu). IR (KBr, cm^{-1}): 3322 (NH), 3350–3100 (w, br, υOH), 1733, 1717 (s, υ C=O), 1616 (s, υ C=O amide I), 1539 (s, δ_{NH} amide II). UV (CH_3OH): λ_{max} = 446 nm, ε = 401 cm^{-1} M^{-1}.

Preparation and characterization of G2OH

G2OEt (0.65 g, 1.2 m*M*), NaOH (500 mg, 6 m*M*), (R_f = 0.20 AcOH/MeOH/$CHCl_3$ 1 : 2 : 17 giving an orange solid. Yield: 0.33 g, 52%. FAB-MS: MW calculated for $C_{26}H_{31}N_3O_{11}Fe$ = 618.1386 $[M+1]^+$, found: 619.1398. ^{1}H NMR (δ in ppm DMSO-d_6): 12.58–12.10 (4H, m, OH), 8.17 (2H, d, J = 4.0 Hz, NH), 7.84 (1H, d, J = 13.0 Hz, NH), 4.26, 4.22 (3H, m, CH^{α}-Glu.), 4.90 (1H, s, H^o Cp), 4.81 (1H, s, H^o Cp), 4.35 (2H, s, H^m Cp), 4.24 (5H, s, Cp), 2.23–2.33 (6H, m, CH_2^{γ}-Glu), 2.00–1.91 (6H, m, CH_2^{β}-Glu). ^{13}C NMR (δ in ppm, DMSO-d_6): 174.7–170.1 (C-carbonyl), 76.8 (quaternary C-substituted Cp), 70.9 (C^o-Cp), 70.3 (C-unsubstituted Cp), 69.3 (C^m-Cp), 53.3, 52.0, 49.5 (CH^{γ}-Glu), 32.7–27.2 (CH_2-Glu). IR (KBr, cm^{-1}): 3322 (NH), 3350–3100 (w, br, υOH), 1716 (s, υ C=O), 1633 (s, υ C=O amide I), 1530 (s, δNH amide II). UV (CH_3OH): λ_{max} = 442 nm, ε = 350 cm^{-1} M^{-1}.

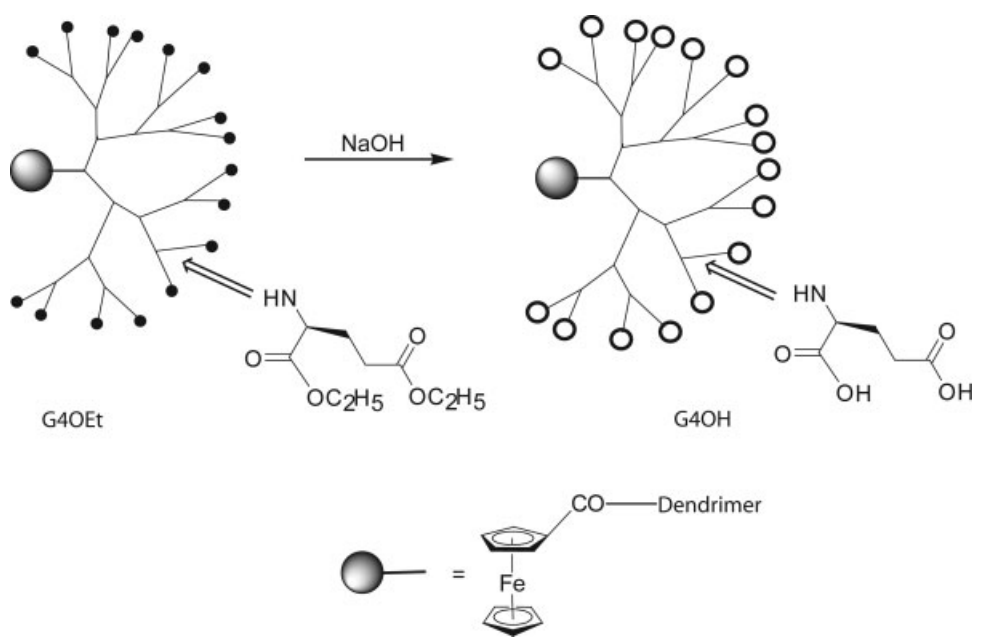

Scheme 1 Sketch of the synthesis of carboxylate terminal dendrimer G4OH from its G4OEt analogue and position of the Fc moiety with respect to the general dendrimer architecture.

Preparation and characterization of G3OH

Compound **G3OEt** (1.1g, 3.0 m*M*), NaOH (100 mg, 2.4 m*M*), (R_f = 0.20 AcOH/MeOH/$CHCl_3$ 1 : 2 : 17, orange solid. Yield: 75%. FAB-MS: MW calculated for $C_{46}H_{60}N_7O_{23}Fe$ = 1134.3090 $[M+1]^+$, found: 1134.3107. ^1H NMR (δ in ppm, DMSO-d_6): 13.89–11.80 (broad peak, OH), 8.77–7.91 (7 H, NH), 4.15, 4.71 (7H, m, CH^{α}-Glu.), 4.91 (2H, H^o Cp), 4.95 (2H, H^m Cp), 4.25 (5H, Cp), 2.50–1.36 (32H, CH_2-Glu). ^{13}C NMR (δ in ppm, DMSO-d_6): 175.2–170.4 (C-carbonyl), 76.6 (quaternary C-substituted Cp), 70.9 (C^o-Cp), 89.5 (C-unsubstituted Cp), 69.3 (C^m-Cp), 54.3–52.2 (CH^{α}-Glu), 32.6–23.3 (CH_2^{γ}-Glu). IR (KBr, cm^{-1}): 3322 (NH), 3350–3100 (w, br, υOH), 1721, (s, υ C=O), 1659 (s, υ C=O amide I), 1536 (s, δNH amide II). UV (CH_3OH): λ_{max} = 449 nm, ε = 170 cm^{-1} M^{-1}.

Preparation and characterization of G4OH

Compound **G4OEt** (1.8 g, 0.7 m*M*), NaOH (450 mg, 11.32 m*M*); yield: 26%. FAB-MS: MW calculated for $C_{86}H_{116}N_{15}O_{47}Fe$ = 2167.6576 $[M+1]^+$; found: 2167.4831. ^1H NMR: (δ in ppm, DMSO-d_6): 12.40–11.30 (broad, OH), 8.59–7.78 (15 H, NH), 4.71–4.13 (15H, m, CH^{α}-Glu.), 4.33 (2H, H^o Cp), 4.88, 4.67 (2H, H^m Cp), 4.18 (5H, Cp), 2.36–1.36 (64H, CH_2-Glu). ^{13}C NMR (δ in ppm, DMSO-d_6): 174.5–169.7 (C-carbonyl), 76.7–70.2 (C-Cp), 69.2 (C^m-Cp), 62.4–51.2 (CH^{α}-Glu), 35.1–25.4 (CH_2-Glu). IR (KBr, cm^{-1}): 3322 (NH), 3350–3100 (w, br, υOH), 1738 (s, υ C=O), 1656 (s, υ C=O amide I), 1536 (s, δNH amide II). UV (CH_3OH): λ_{max} = 416 nm, ε = 255 cm^{-1} M^{-1}.

Preparation and characterization of G5OH

Compound **G5OEt** (0.3 g, 0.07 m*M*), NaOH (83 mg, 2.08 m*M*), yield: 62 % FAB-MS: MW calculated for $C_{166}H_{227}N_{31}O_{63}Fe$ = 3719.4895 $[M+1]^+$, found: 3719.6889. ^1H NMR (δ in ppm, DMSO-d_6): 12.40 (broad, OH), 8.18–7.84 (31H, m, NH), 4.81–4.24, 386–3.33 (31H, m, CH-Glu.), 4.87, 4.83 (Cp), 4.18 (5H, Cp), 2.30–2.06 (124H, m, CH_2-Glu). ^{13}C NMR (δ in ppm, DMSO-d_6): 174.0–172.3 (C-carbonyl), 69.9–68.0 (C-Cp), 52.7–51.1 (CH^{α}-Glu), 32.1–26.5 (CH_2^{γ}-Glu). IR (KBr, cm^{-1}): 3322 (NH), 3350–3100 (w, br, υOH), 1738 (s, υ C=O), 1650 (s, υ C=O amide I), 1533 (s, δNH amide II). UV (CH_3OH): λ_{max} = 413 nm, ε = 225 cm^{-1} M^{-1}.

LbL multilayer assembly

Films of 11-mercaptoundecanoic acid (MUA) were prepared by placing a Au electrode (BAS, area 0.02 cm^2) in 5.0 m*M* MUA in ethanol for 48 h, followed by thorough rinsing with ethanol and water. The freshly prepared MUA film was then immersed in a 2.0*M* $NaClO_4$ solution (pH = 6.8) for 15 min, followed by rinsing with deionized water. The film-modified electrodes were then immersed in aqueous 5.0 m*M* metal ion solution for 20 min. After rinsing with water, ethanol and drying with N_2 gas, the metal functionalized film was immersed in 1.0 m*M* aqueous solution of the Fc-dendrimer G(n)OH for 20 min. The process was repeated each time as outlined in Scheme 2.

RESULTS AND DISCUSSIONS

Prior to LbL deposition, MUA films on gold, serving as a sublayer, were characterized by cyclic voltammetry (CV) using with $[Fe(CN)_6]^{3-/4-}$ as a solution redox probe at pH 6.8.[50–52] Figure 1 shows a typical CV of the gold surface before and after MUA modification. At the bare gold surface, the cathodic and anodic peaks, assigned to the reduction and oxidation of the $[Fe(CN)_6]^{3-/4-}$ couple were observed at a $E_{1/2}$ = 190 mV (vs. Ag/AgCl), with a peak separation ΔE = 95 mV and peak current ratio i_{pa}/i_{pc} of unity. The values of ΔE and i_{pa}/i_{pc} indicate a quasi-reversible redox behavior. In contrast, the MUA film shows a significantly reduced Faradaic current, indicating a lack of permeability of the film towards the redox probe. This is readily rationalized considering the electrostatic repulsion between the probe and the surface at pH 6.8.[53–56]

Multilayer metal-dendrimers formation

Alternating layers of metal ions and dendrimer acids G1OH–G5OH were deposited onto the MUA sublayer at pH 6.8 as illustrated in Scheme 2. CVs and DPVs were recorded for metal-terminated and dendrimer-terminated layers after each "dip and wash cycle" at scan rate of 100 mV s^{-1} in 2.0*M* $NaClO_4$ and used to monitor and evaluate the electrochemical response of the film. At this pH, the metal ions are expected to coordinate to the MUA carboxylate group. Prior work by Ulman showed that a number of cations (Cd^{2+}, Pb^{2+}, Ba^{2+}, and Ca^{2+}) form dense ionic overlayers on MUA films.[57] The construction of bilayers of $[M^{n+}/G(n)OH]n$ films on MUA-Au electrodes was monitored by CV. When the first bilayer of MUA/M^{n+} was immersed in a solution of the dendrimers G(n)OH at pH 6.8, a pair of well defined and quasi-reversible characteristic of one electron transfer of Fc/Fc^+ redox couple was observed with formal potential in the range from 419 mV to 472 mV which is typical of peptide mono-substituted substituted ferrocene monolayers.[46,47] Figure 2 shows a CV stack plot of [Tb/G2OH]n and [Ca/G2OH]n for six layers each of Tb^{3+} and Ca^{2+} ions and G2OH. Although the first Tb^{3+}/Ca^{2+} on MUA-Au electrode exhibited no redox activity in the

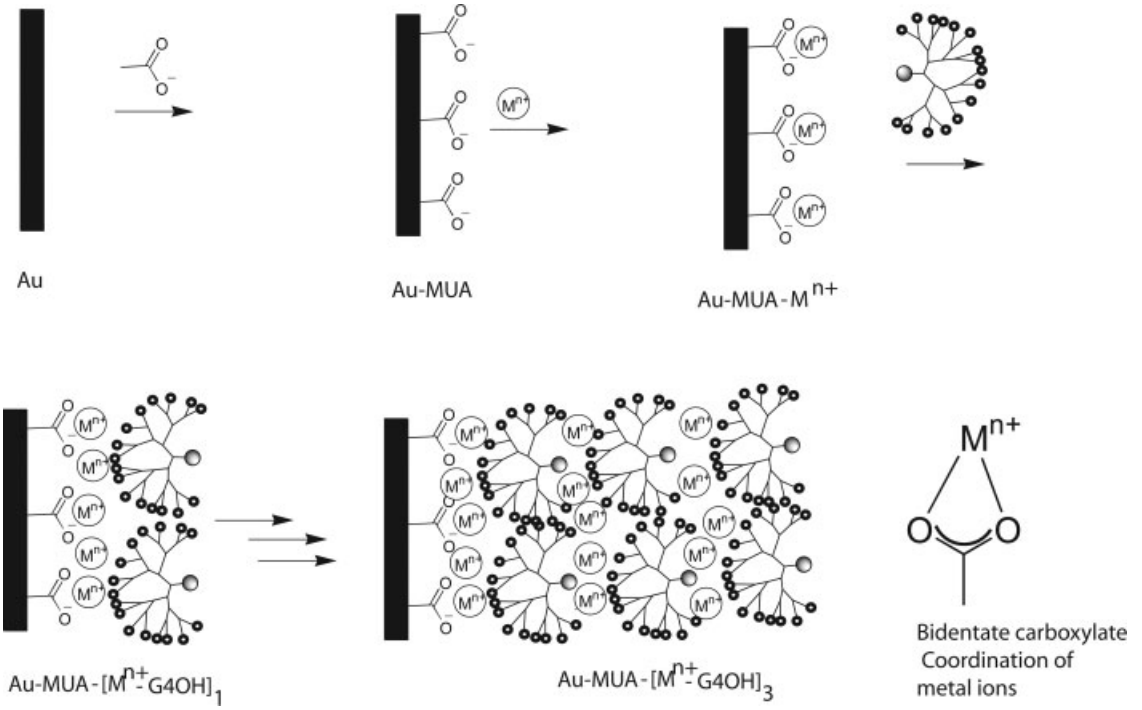

Scheme 2 Schematic view the preparation of the LbL film involving alternating layers of dendrimer and metal ions on a 11-mercaptoundecanoic acid sublayer.

experimental potential window, the coordination of the metal ions with the carboxylate group of the dendrimers forming an Au-MUA/Tb^{3+}or Ca^{2+}/G2OH film resulted in observance of the Fc/Fc^{+} redox peak. The addition of a second layer of Tb^{3+}/Ca^{2+} results in a decrease in the peak current of the Fc/Fc^{+}redox peak while addition of second layer of G2OH not only restored the peak but also an addition increase in the current was observed. The results after six layers of Tb^{3+}/Ca^{2+} and G2OH layers reveal a dependence of the reduction peak current on the nature of the outermost layer. The results showed that when the bilayers of $[M^{n+}/G(n)OH]_n$ films had a M^{n+} outermost layer the peak current decreased drastically compared to the original film. However in the next G2OH adsorption step, the peak current increased than the previous films. Thus, the reduction peak current of the films switched between higher and lower levels depending on the component of the outer layer and demonstrate a general trend of increase in peak current with number of adsorption layers. Similar trends were observed with other dendrimers generations and with a change in metal content. However, the magnitude of the peak current was dendrimer generation dependent as well as nature of interlocking metal ion dependant. Generally films with Tb^{3+} ion showed higher peak currents compared to films with Ca^{2+} ion (Fig. 2) while in terms of dendrimer generations the sequence G2OH > G3OH > G1OH $\gg$ G4OH > G5OH was observed.

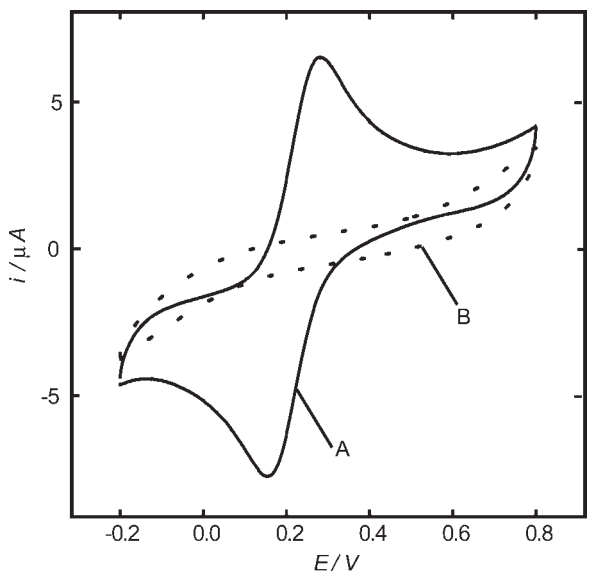

Figure 1 (A) CV of the bare gold and (B) MUA SAM in the presence of $[Fe(CN)_6]^{3-/4-}$ versus Ag/AgCl in 2.0*M* $NaClO_4$ at pH 6.8.

Generally coordination numbers is 8–12 and 6–8 for lanthanide-carboxylate complexes and alkaline earth metals, respectively. This difference should have significant influence on the number of molecules of Fc dendrimers adsorbed per layer. The

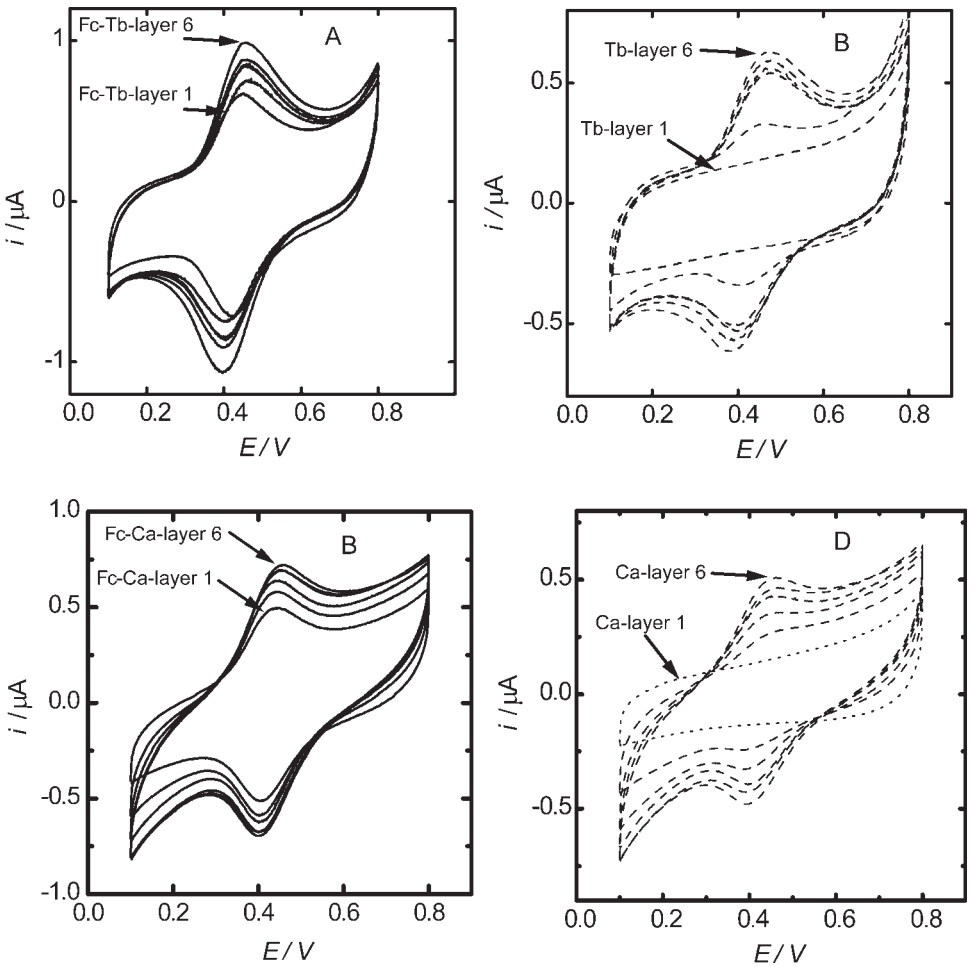

Figure 2 CVs stack plots of G2OH-Tb multilayer with the Fc as outermost layers (A), with the Tb^{3+} as outermost layers (B); and CVs stack plots of G2OH-Ca multilayer with the Fc as outermost layers (C), with the Ca^{2+} as outermost layers (D) in 2.0*M* $NaClO_4$ at pH 6.8 versus Ag/AgCl.

change in peak current is better represented by DPV scans of the multilayers as represented for G1OH-Tb system in Figure 3. The formal potential of M^{n+}G(n)OH bilayer shifts slightly anodically as the number of generation increases. For example, a comparison of the first layers of the Tb^{3+} and Ca^{2+} with Fc outermost layer becomes more positive as we increase the generation size of the dendrimer (Table I). For a given multilayer sequence, the formal potential also increased slightly with each additional layer, a situation that has been observed for ferrocene-tethered polyamidamine dendrimer and polyallyamine ferrocene-glicose oxidase multilayers.[10,30] The increases were more pronounced in higher generations as compared to lower generations. The peak-to-peak separation ΔE were small and less than 90 mV (at 100 mV s^{-1}) which shows a fast electron transfer kinetics across the length of the multilayer by electron hopping between adjacent redox centers of the multilayer matrix. Full width at half maximum (E_{fwhm}) expected for an ideal one electron Nernstian redox system is 90.6 mV for the case of a non-interactions between adsorbates. The observed values in the range of 120–136 mV for lower generations are indicative of non-uniform packing and the existence of repulsive interactions between the redox sites. This is however not unexpected because the 3D packing of the adsorbates would lead to more interactions between the Fc redox centers more especially with the lower generations. For higher generations however, the values are as expected and show that the Fc redox centers are uniformly packed and show no interactions between redox centers. Higher generations of redox core dendrimers has been shown to adopt globular conformations, encapsulating the probe and thus prevents interactions of adjacent redox core in the multilayers.

To investigate the charge transport within the multilayered metal glutamic acid dendrimers on various films, we measured the plots of anodic and cathodic peak current (i_p) as the scan rate increased (Fig. 4). The results show that i_p increased with scan rate which is consistent with surface adsorbed electroactive systems and indicative of the formation of

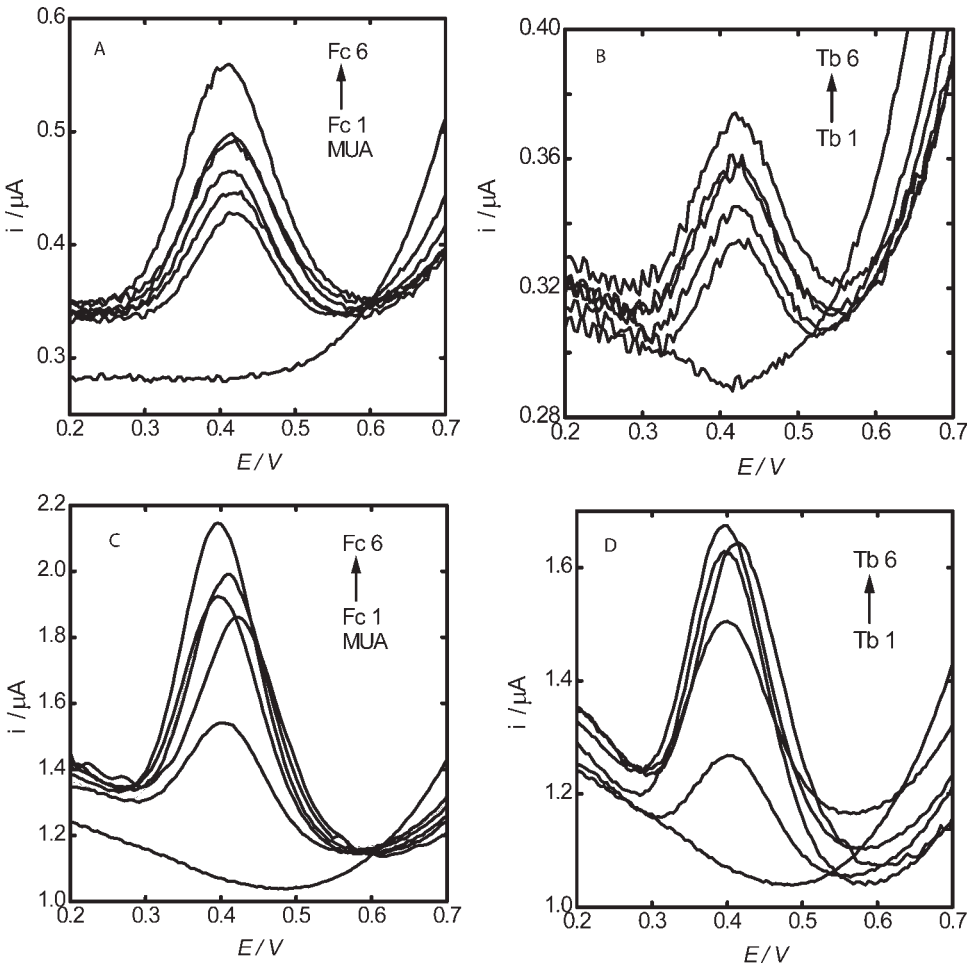

Figure 3 DPVs stack plots of G1OH-Tb multilayer with the Fc as outermost layers (A), with the Tb^{3+} as outermost layers (B); and DPVs stack plots of G3OH-Tb multilayer with the Fc as outermost layers (C), with the Tb^{3+} as outermost layers (D) in 2.0*M* $NaClO_4$ at pH 6.8 versus Ag/AgCl.

very stable layers that did not involve diffusion-like transfer to the electrode. There is almost no change in ΔE with change in scan rate, implying that the electron transfer between the Fc redox sites and the electrode is fast. Significantly, the six layered films were as stable as the monolayered films of the dendrimers on the Au-MUA films. The faradaic charge associated with ferrocene-ferrocenium electron transfer process was determined by integrating the area under the peak of the CVs from which the surface

TABLE I
Electrochemical Data from CV of MUA/(G(n)OH-M^{n+})$_n$ for First and Last Layer Films Assembled on MUA Electrode with Fc-as Terminal Layers at 100 mV s^{-1} in 2.0*M* $NaClO_4$ at pH 6.8 versus Ag/AgCl

	MUA/Tb^{3+}			MUA/Ca^{2+}		
	E^o	ΔE	ΔE_{FWHM}	E^o	ΔE	ΔE_{FWHM}
(G1OH-M^{n+})$_1$	436 ± 8	44 ± 15	128 ± 5	419 ± 18	39 ± 12	129 ± 6
(G1OH-M^{n+})$_6$	439 ± 12	52 ± 10	137 ± 8	435 ± 15	52 ± 8	125 ± 5
(G2OH-M^{n+})$_1$	425 ± 10	34 ± 10	140 ± 4	424 ± 12	40 ± 14	120 ± 8
(G2OH-M^{n+})$_6$	438 ± 12	55 ± 12	157 ± 4	429 ± 14	38 ± 12	139 ± 6
(G3OH-M^{n+})$_1$	428 ± 14	66 ± 10	120 ± 6	424 ± 16	51 ± 14	121 ± 9
(G3OH-M^{n+})$_6$	451 ± 14	55 ± 12	136 ± 5	448 ± 10	81 ± 18	131 ± 6
(G4OH-M^{n+})$_1$	465 ± 10	26 ± 14	101 ± 8	458 ± 14	45 ± 15	99 ± 5
(G4OH-M^{n+})$_6$	479 ± 15	30 ± 16	103 ± 4	469 ± 13	55 ± 14	106 ± 8
(G5OH-M^{n+})$_1$	477 ± 13	31 ± 10	96 ± 6	472 ± 13	67 ± 17	95 ± 6
(G5OH-M^{n+})$_6$	479 ± 12	28 ± 10	101 ± 3	480 ± 15	77 ± 18	102 ± 6

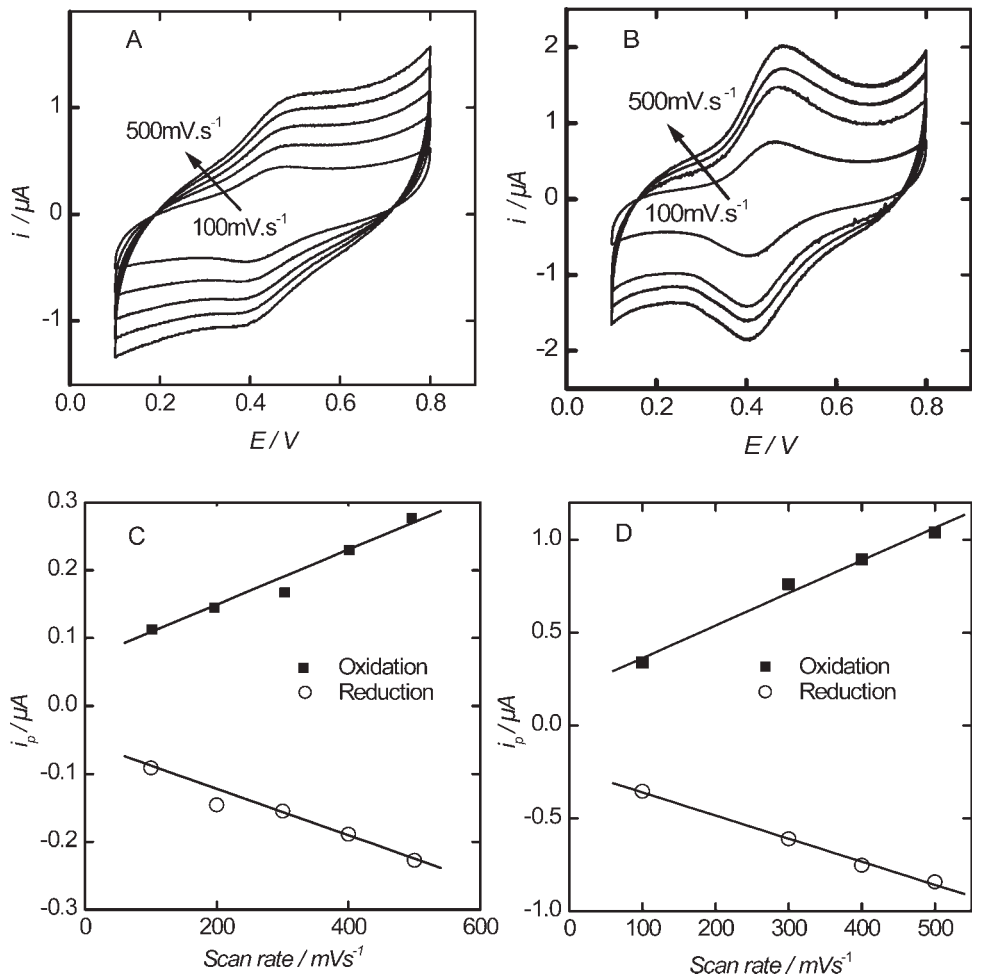

Figure 4 CV of G2OH-Tb1 (A) and G2OH-Tb6 (B) with increasing scan rates. Dependence of anodic and cathodic peak currents as the scan rate is increased for G2OH-Tb1 (C) and G2OH-Tb6 (D) in 2.0*M* $NaClO_4$ at pH 6.8 versus Ag/AgCl.

coverage of active ferrocene derived. The surface coverage Γ is given by,

$$\Gamma = Q/nFA$$

where Q is the charge associated with the redox activity, n is the number of electrons (in this case $n = 1$), F the Faraday's constant, and A is the area of the electrode.

The estimated average surface concentration of active Fc as shown in Figure 5 oscillated as a function of the number of alternate layers of the metal ion and dendrimers for all generations. The decrease in redox charge as one changes from a Fc-dendrimer terminal to metal ion terminal may be due to some Fc being desorbed from the surface into the electrolyte or to some hindrance of a fraction of the Fc sites from oxidizing and reducing. Similar trends have been observed for LbL of cationic poly(allamine) modified with Os and anionic poly(styrene)sulfornate (PSS) or poly(vinyl)sulfornates) PVS,[31] charged enzymes or proteins over oppositely charged polymers.[7] Wang and Schlenoff have shown for viologen systems with radiolabeled polyelectrolytes that there was no desorption of polymers from the surface when immersing the electrodes in solution of the oppositely charged polyelectrolytes.[58] The oscillating coverage with layers of terminal Fc and metal is also consistent with the ion pair effect originally proposed separately by Creager and Uosaki who noted that the redox process of surface attached ferrocene group is significantly affected by the interaction of the counterion and the ferrocene moiety.[59,60] For most of the systems studied, when the number of layers exceeded 4, little increase in peak current and Γ was observed (Tables II and III), indicating that some of Fc in the bilayers beyond this limit were not electroactive. The Γ value increased nonlinearly with increase in layers up to the 6th bilayer. Assuming the first bilayer is assigned arbitrarily as 100% electroactive species, and taking the results for G2OH as a hypothetical case, one would expect that the five bilayer would increase considerably, but the fraction of electroactive Fc added to all the film systems drastically

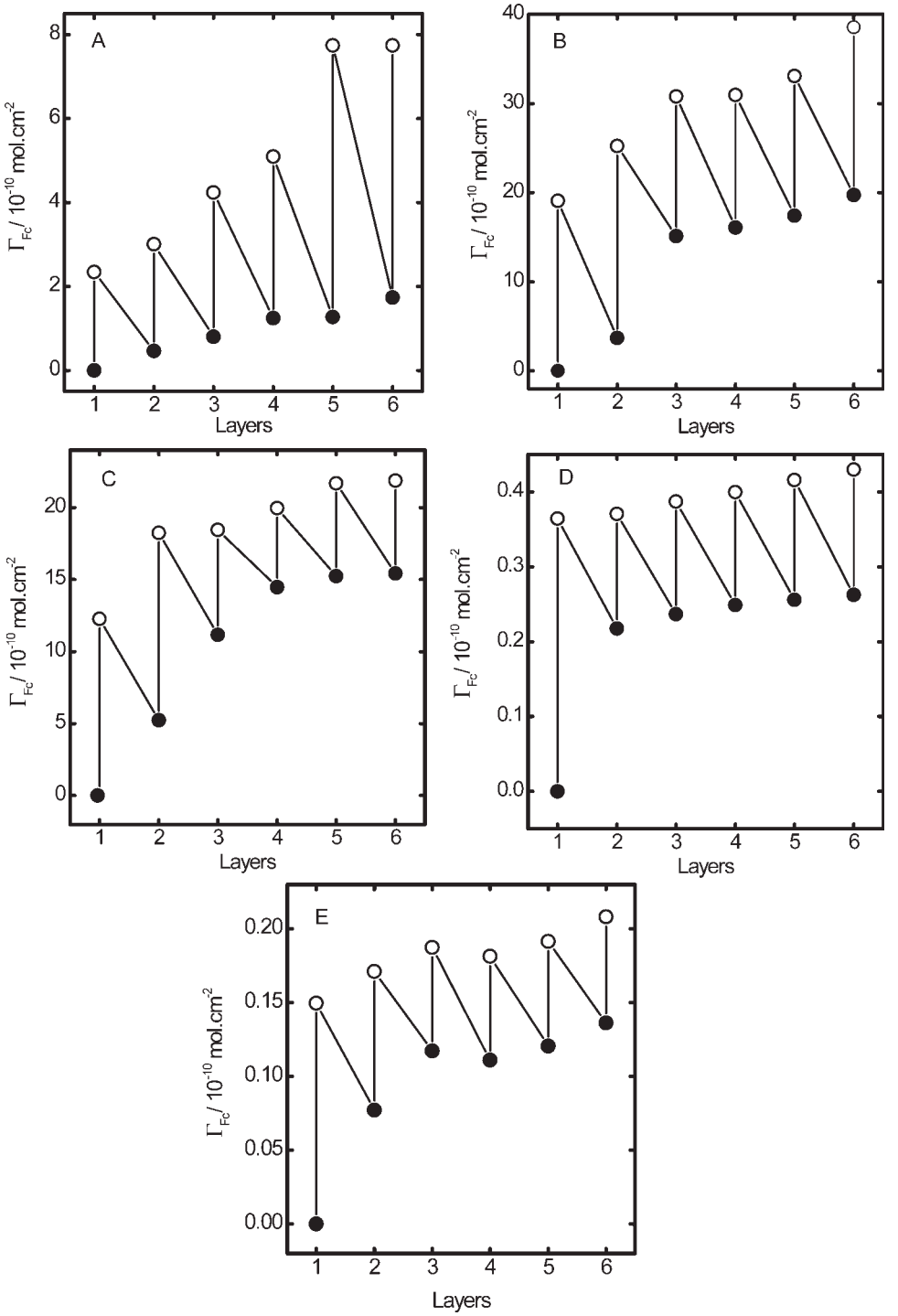

Figure 5 Plots of oscillation trend surface coverage of active Fc for alternating layers of G1OH (A), G2OH (B), G3OH (C), G4OH (D), G5OH (E) with Tb. Metal terminated layers (●) and dendrimer terminated (○).

reduced with each added bilayer. This is may be indicative of the fact that the distance between the Fc moiety in the films and the electrode is a necessary factor in electron transfer through these systems,[61–64] or that the orientation of molecules of subsequent layers do not allow for sufficient electron transfer between the redox Fc and the electrode.

A comparison of increase in surface concentration of active Fc for the dendrimers with the two metals indicated the G2OH > G3OH > G1OH ≫ G4OH > G5OH as observed for peak currents. This trend though surprising can arise from a variety of reasons; theoretical and experimental studies of dendrimers have been shown to have the tendency to

flatten and spread out on substrates when interfacial interactions are strong.[65,66] They prefer to adopt conformations that balances the entropy factor that favor spherical shape and the enthalpy factor that tends to maximize the interactions with the substrates and thus compresses the molecule.[67]

Film deposition of dendrimers deform and adopt to shape of the electrode as reported in the case of surface adsorption of poly(amido)amine dendrimers.[68,69] Micelle-mimetic behavior of dendrimers has been observed in recent molecular dynamic studies. Depending on the conditions of the bulk solution, i.e., its polarity, ionic strength, and pH, dendrimers adopt conformations of different shape and density. As a result of these interactions, polar dendrimers will have a higher density at the core in poor (apolar) solvents and a higher density at the surface in good (polar) solvents.[70] For this reason, higher generations G4OH and G5OH may be denser at their surfaces thereby encapsulating the redox core to a greater degree and cutting off the interaction with the electrode. Electron transfer also involves tunneling of electrons across the dendritic sheath. Because the rate of electron transfer is related to the donor-acceptor distance, it can be expected that increasing dendrimer size will influence the kinetics of electron transfer process and thus the observed lower surface activity of the higher generations. The greater activity of G2OH, G3OH compared to G1OH may be a result of their orientation on the layers such that they have more terminal ligands that are available for coordination with the upper metal layers than that of the lower G1OH thus favoring easy electron transfer with the electrode beneath. The electron transfer in the lower generation G1OH may also be a result of low packing densities in the polymer.[10]

Contribution of hydrogen bonding to multilayer metal-dendrimers formation

Peptide dendrimers contain both carboxylate and amide linkages which are known to enable hydrogen bonding interactions. In polymeric frameworks of solid-state X-ray structure of calcium-carboxylate coordination polymers strong hydrogen-bonding interactions between the coordination polymers forming a network have been reported. The calcium layer is held together by strong interlayer hydrogen bonds between carboxylate and aqua ligands to yield a tightly held stabilized three-dimensional structure. Such networks include the complexes of carboxyphenyl-porphyrin, the terephthalate, succinate napthalenetetracarboxylate, phthalate, glycerate, glutamate, and 1,3,5-benzenetricarboxylate[71–78] ions. The question therefore arises as to the contribution of hydrogen bonding to the formation of multilayers at the prevailing experimental condition in the absence of the intervening metal ions.

To address this concerns, we have also investigated the formation of multilayers in the absence of the interspaced metal ions using the G2OH system. Figure 6 shows the CVs of carboxylate-terminated Au electrode, modified by G2OH at pH 6.8 carried out by the dip and dry sequence without the interspacing metal layers. The redox formal potential was 425 mV and 440 mV for the first and sixth layer, respectively, which is similar to that observed for the Tb^{3+} and Ca^{2+} assisted systems. This indicates that the presence of the metal ions had very little effect on the electrode formal potential on surface immobilized Fc peptide in contrast to the situation in solution-based ion interactions.[79,80] In the latter situation, the M^{n+} experiences a repulsion in the presence of the oxidized Fc^{+} species whereas in the immobilized state such effects are not uncounted in view of the formation of the $Fc^{+}/ClO_3{}^{-1}$ ion pair.

Scanning at various scan rates at the sixth layer shows that the anodic and cathodic peak currents are proportional to the scan rate for scan velocities up to 500 mV s^{-1}. The proportionality between current and the scan rate reflects the reversibility of the redox probe and as before a surface confined stable multilayer is formed in the presence of hydrogen bonding. The peak potential difference ΔE is 81 mV and remained constant during the variation in the scan rate indicating a fast electron transfer. As shown in Figure 6, the CV's shows a much reduced peak current for the first three layers followed by a shape increase in the peak current after the fourth layer. As the two —COOH groups of the parent glutamic acid have pK_a values of 2.19 and 4.33, while that for polyglutamic acid is 5.41[81] and MUA monolayer pK_a is 5.2–6.4, all of the COOH termini of the MUA and G2OH are expected to be deprotonated at pH 6.8 to afford a surface negative charge. It is therefore understandable to expect small adsorption of the first few layers as compared to the systems have interlocking metal because of repulsion between the dendrimer and the MUA interface the former and charge neutralization in the metal multilayer cases. After the 4th layer, however, the significant contribution of hydrogen bonding possibly from the amide-carbonyl interaction becomes more predominant leading to highly stable multilayer system as shown by perfect reversible the CV of the 6th layer with its linear plot of scan rate.

Although the pK_a values of the carboxyl group of the Glu are different in the dendritic chain, they are all in the range of 2–5. Thus at pH 6.8, the surface are negatively charged but the amide NH and C—O groups may be involved in the hydrogen bonding. Multilayer of amine terminated PAMAM dendrimers with Pt^{2+} [35] have been shown not to be

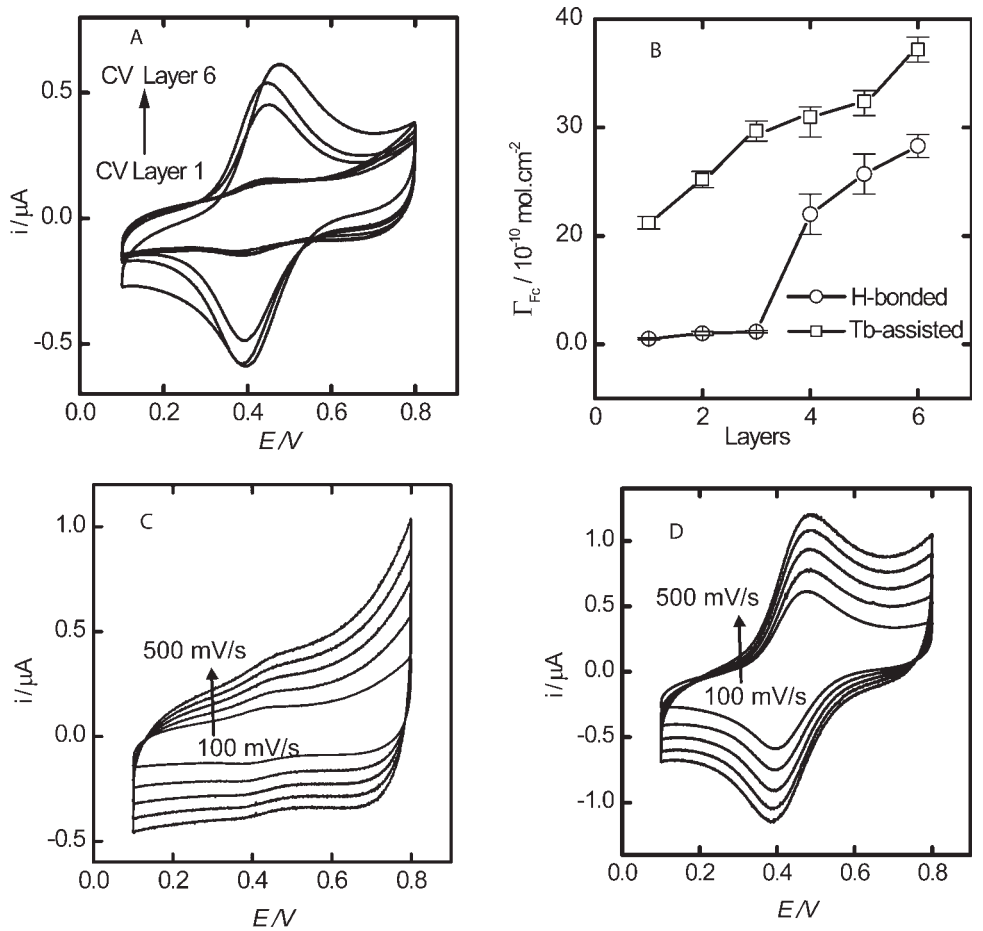

Figure 6 (A) Layer deposition of G2OH on MUA at pH 6.8. (B) Comparism of Γ for G2OH at pH 6.8 with Tb^{3+} and without the metal interlocking layers of deposition. (C) CV of the 1st layer of G2OH at various scan rates, (D) CV of the 6th layer of G2OH without metal layers at various scan rates.

possible when the metal activation cycle was eliminated. Rubinstein and coworkers have demonstrated the binding of chromophore protoporphyrin layers on MUA monolayers with or without binding Cu^{2+} to the MUA monolayer. They showed that layers were better organized and coverage was higher with the use of Cu^{2+} as the intervening layer.[82] Calculation of the surface concentration of the active ferrocene derived from the CVs indicates an initial lack of growth for the first few layers followed by a sudden rise (Fig. 6B). This may be explained in terms of the lack of effective buildup because of the negative charge on the carboxylates moiety. Comparison to that of the metal assisted multilayer formation clearly shows that at higher layers the positive contributory role of hydrogen bonding in the formation of multilayers cannot be ruled out. The lack of initial contribution might stem from the negatively charged MUA interface which at pH 6.8 is expected to be negatively charged which should then repel the negatively charge carboxylate terminals of the redox active dendrimer. Because no increase in redox response was observed if the dipping solution contained no metal ions, at least for the first few layers, it may demonstrated that electrostatic interactions was essential for the construction of well-defined multilayers of dendrimers. Moreover, metal multilayers with 1,3,5-tricarboxylic benzoic acid (trimesic acid, TMA), 1,4-benzenedicarboxylic acid (terephthalic acid, TPA), 1,2,4-benzenetricarboxylic acid molecules (trimellitic acid, TMLA), and 4,1′,4′,1′′-terphenyl-1,4′′-dicarboxylic acid (TDA). TMA, TPA, and TMLA have an aromatic ring (three aromatic rings for TDA) as backbone and all four have carboxylic groups as functional end groups chains anchored by the metal ions are stable at room temperature, which reflects the appreciable strength of metal–ligand interactions that exceed hydrogen-bonding interactions of their polymers.[83,84]

Effect of non-redox intervening dendrimer layers on electron transfer

Schlenoff et al. have shown that electron transfer through multilayer films was via electron hopping between neighboring sites which is facilitated by

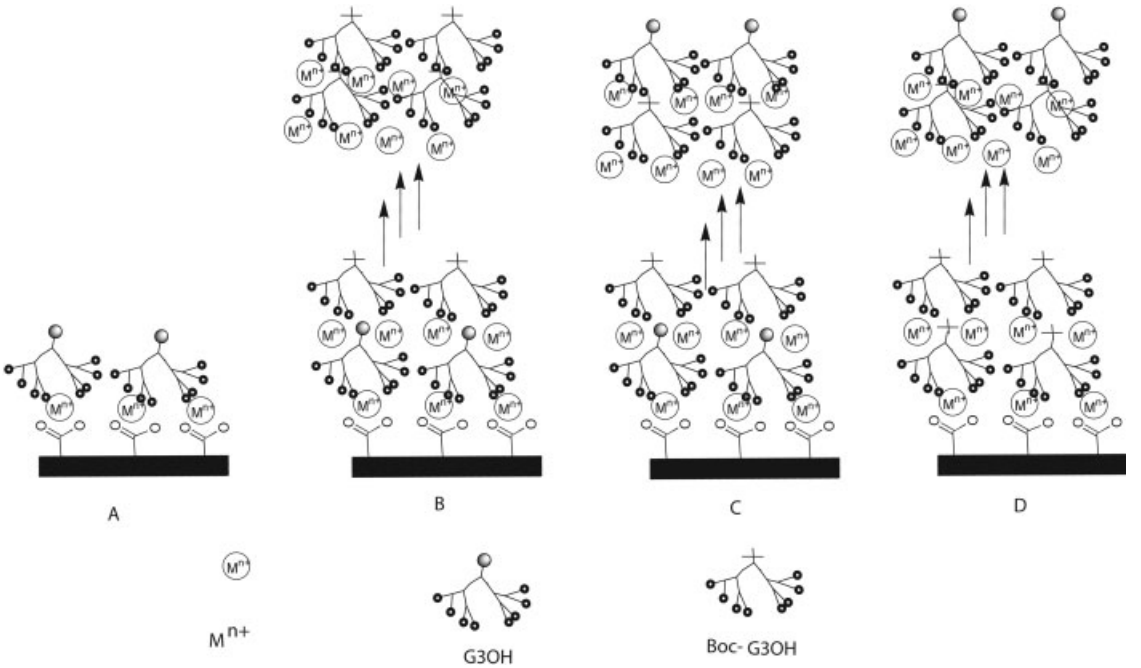

Scheme 3 Illustration of (A) Au-MUA-Tb^{3+}-G3OH, (B) Au-MUA-Tb^{3+}-G3OH-(Tb^{3+}-Boc-G3OH)$_5$, (C) Au-MUA-Tb^{3+}-G3OH-(Tb^{3+}-Boc-G3OH)$_4$-Tb^{3+}-G3OH, (D) Au-MUA-(Tb^{3+}-Boc-G3OH)$_5$-Tb^{3+}-G3OH multilayer systems.

interpenetrating of alternate layers.[85,86] According to Schlenoff, upon reduction a negative charge is introduced into the multilayer and this is compensated by the intake of positive ions which they proved with the use of $^{45}Ca^{2+}$ in solution.[87] Studies by Uosaki and coworkers on multilayer of gold nanoclusters (MG), ferrocenylhexanthiol-gold nanocluster (MGF), and polycation polyallylamine on MUA-Au electrode or Cu^{2+} ion have shown that a quasi reversible redox peak with a constant charge corresponding to the redox reaction of the ferrocene was observed whether the MGF was placed closest to the electrode (first layer) or on the outermost layer.[88–90] They conclude that this happens because electrons are transferred between the ferrocene moiety and the electrode whereas the perchlorate ions are transferred between the electrolyte solution and the ferrocene moiety through the multilayer by ion-pair formation.

To have an idea of the distance requirement for the observation of redox activity, we used the ferrocene functionalized G3OH (because it is the largest dendrimer that exhibited significant Γ) and the Boc protected analogue Boc-G3OH together with Tb^{3+} ion on MUA-Au electrode as illustrated in Scheme 3 ((A) Au-MUA-Tb^{3+}-G3OH, (B) Au-MUA-Tb^{3+}-G3OH-(Tb^{3+}-Boc-G3OH)$_5$, (C) Au-MUA-Tb^{3+}-G3OH-(Tb^{3+}-Boc-G3OH)$_4$-Tb^{3+}-G3OH, (D)Au-MUA-(Tb^{3+}-Boc-G3OH)$_5$-Tb^{3+}-G3OH). Figure 7(A–D) shows the CV scans at a rate of 100 mV s^{-1} measured in 2.0*M* $NaClO_4$ at pH 6.8 versus Ag/AgCl for the system illustrated in Scheme 3. From comparing CV (A) to CV (B), we observed no redox activity in the latter indicating no activity beyond the second Boc layer contrail to the observations by Uosaki group. Replacing the topmost Boc layer by a Fc layer (C) shows that the peak is not only restored but also increased in peak current as observed for the multiple G3OH layers. This may suggest an interpenetrating layer in the presence of the two layers or a distance sufficient enough for electron hopping between the two Fc layers. In the case of (D) the peak current is not too different compared to (A) as can be observed from both the CV and the DPV scans. There is however a significant difference in the charging current which relates to the double layer between the electrode and the redox moiety. Schlenoff showed that for topmost poly(styrenesulfonate) and poly(butanylviologen) (PBV/PSS) layer, interspersed by PAH (non-electroactive)/PSS on Au functionalized with 3-mercapto-1-propanesulphonic acid, redox signals was not observed with four PAH/PSS layer pairs but a redox peak was observed

TABLE II
Surface Concentration of Fc Derived from CV of MUA/(G(n)OH-Tb^{3+})$_n$ for First and Last Layer Films Assembled on MUA Electrode with Fc-as Terminal Layers Γ/10^{-10} mol cm^{-2}

	G1OH	G2OH	G3OH	G4OH	G5OH
(G(n)OH-Tb^{3+})$_1$	2.34	19.1	12.67	0.36	0.15
(G(n)OH-Tb^{3+})$_2$	3.00	25.23	18.24	0.37	0.17
(G(n)OH-Tb^{3+})$_3$	4.23	30.79	18.45	0.39	0.19
(G(n)OH-Tb^{3+})$_4$	5.08	30.91	19.96	0.31	0.18
(G(n)OH-Tb^{3+})$_5$	7.73	33.09	21.69	0.42	0.19
(G(n)OH-Tb^{3+})$_6$	7.74	38.54	21.87	0.43	0.21

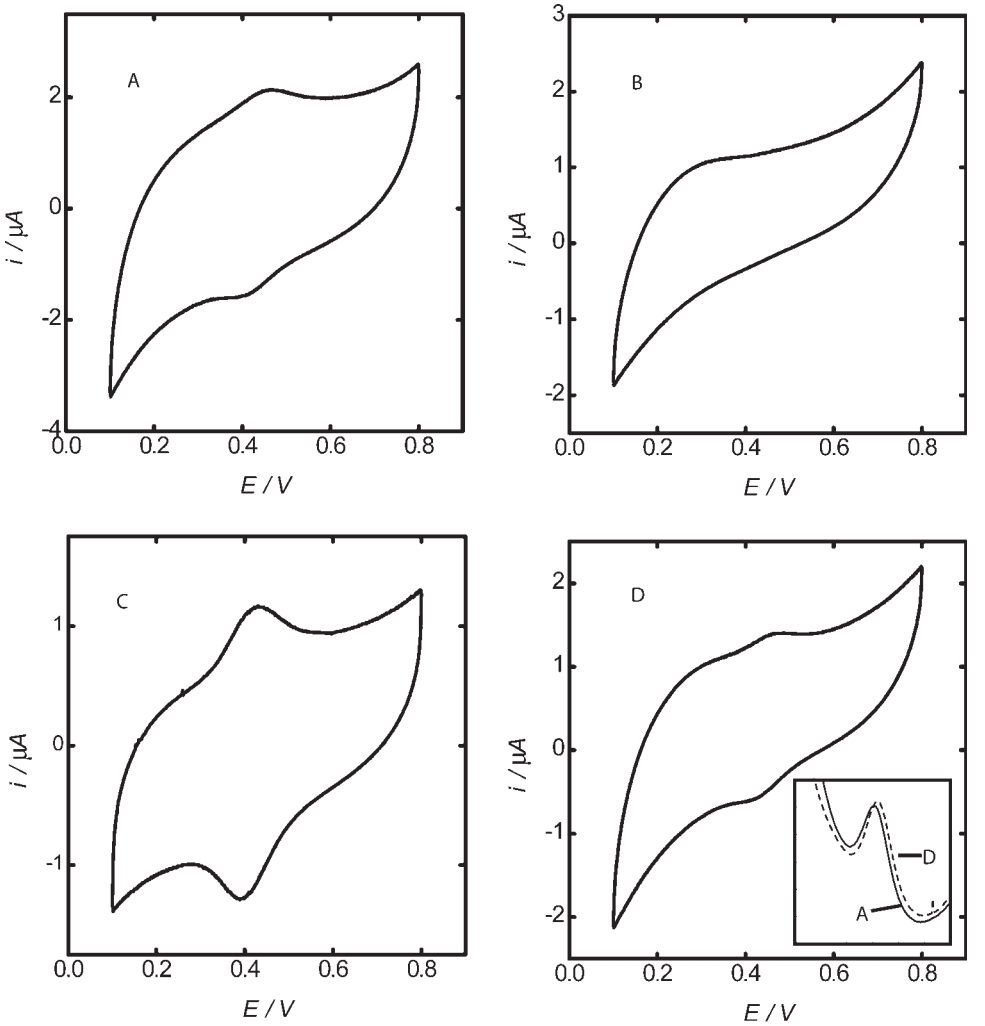

Figure 7 CV scans of (A) Au-MUA-Tb^{3+}-G3OH, (B) Au-MUA-Tb^{3+}-G3OH-(Tb^{3+}-Boc-G3OH)$_5$, (C) Au-MUA-Tb^{3+}-G3OH-(Tb^{3+}-Boc-G3OH)$_4$-Tb^{3+}-G3OH, (D) Au-MUA-(Tb^{3+}-Boc-G3OH)$_5$-Tb^{3+}-G3OH scanned at a rate of 100 mV s^{-1} in 2.0*M* $NaClO_4$ at pH 6.8 versus Ag/AgCl. Inset is the DPV scans for (A) and (D).

for three interspersed PAH/PSS layer (about 180 Å thickness).[86,87] The authors argue that though interpenetration has been observed in other multilayers, the degree of interpenetration is high and implies a certain amount of mobility may account for this phenomenon. Taking the thickness of MUA (10-13 Å),[91,92] Tb (1.2 Å),[93] and G3OH (10–15 Å non-symmetrical from Spartan modeling), we obtain a distance of close to 70 Å from the outermost layer to the electrode. We are unable to establish the limit of detecting redox activity at the present time, but we do not envisage such interpenetrating of five Boc/Tb^{3+} layers because Tb^{3+}/glutamic acid composites are generally more extensive. Direct electron transfer is not possible because the distance between the electrode and the fc group is far greater than the tunneling distance.[94]

TABLE III
Surface Concentration of Fc Derived from CV of MUA/(G(n)OH-Ca^{2+})$_n$ for First and Last Layer Films Assembled on MUA Electrode with Fc-as Terminal Layers Γ/10^{-10} mol cm^{-2}

	G1OH	G2OH	G3OH	G4OH	G5OH
(G(n)OH-Ca^{2+})$_1$	8.45	11.42	6.57	0.32	0.19
(G(n)OH-Ca^{2+})$_2$	8.49	14.25	9.25	0.41	0.21
(G(n)OH-Ca^{2+})$_3$	9.32	18.34	10.47	0.49	0.23
(G(n)OH-Ca^{2+})$_4$	10.71	18.82	10.74	0.51	0.22
(G(n)OH-Ca^{2+})$_5$	11.32	19.11	13.03	0.54	0.25
(G(n)OH-Ca^{2+})$_6$	14.26	19.74	11.71	0.59	0.27

CONCLUSION

The data presented demonstrated that supramolecular architecture and nanostructure of LBL films of ferrocene peptide dendrimers multilayers at the surface could be scrutinized by electrochemical measurements. Assemblies stabilized by metal ion coordination using the carboxylate-metal ion coordination chemistry and hydrogen bonding were

addressed. We have shown that the multilayers of ferrocene dendrimers on Au electrodes exhibit fast electrochemical response increase in active redox activity and stability. The observance of dependence of surface concentration with type metal ions, dendrimer type, the nature of the terminating layer and whether there is interlocking metal ions or not supports the view that charge-compensation of counter ions gives these systems their stability. Moreover, the good compatibility of the dendrimer films with metal ions could advance its use in catalysis and nanoparticulates for medical applications.

H.-B. K. is the Canadian Research Chair in Biomaterials.

References

1. Iler, R. K. J. Colloid Interface Sci 1966, 21, 569.
2. Decher, G.; Hong, J.-D. Makromol Chem Macromol Symp 1991, 46, 321.
3. Decher, G. Science 1997, 277, 1232.
4. Li, C.; Mitamura, K.; Imae, T. Macromolecules 2003, 36, 9957.
5. Steiger, B.; Padeste, C.; Grubelnik, A.; Tiefenauer, L. Electrochim Acta 2003, 48, 761.
6. Yang, S.; Li, Y.; Jiang, X.; Chen, Z.; Lin, X. Sensors and Actuators B 2006, 114, 774.
7. Lvov, Y.; Lu, Z.; Schenkman, J.; Rusling, J. F. J Am Chem Soc 1998, 120, 4073.
8. Gu, T.; Hasebe, Y. Biosens Bioelectron 2006, 21, 2121.
9. Arrington, D.; Curry, M.; Street, S. C. Langmuir 2002, 18, 7788.
10. Suk, J.; Lee, J.; Kwak, J. Bull Korean Chem Soc 2004, 25, 1681.
11. Sun, J.; Wang, L.; Gao, J.; Wang, Z. J Colloid Interface Sci 2005, 287, 207.
12. Khopade, A. J.; Caruso, F. Langmuir 2002, 18, 7669.
13. Noguchi, T.; Anzai, J.-I. Langmuir 2006, 22, 2870.
14. Hoekstra, K. J.; Bein, T. Chem Mater 1996, 8, 1865.
15. Hatzor, A.; Moav, M.; Cohen, H.; Matlis, S.; Libman, J.; Vaskevich, A.; Shanzer, A.; Rubinstein, I. J Am Chem Soc 1998, 120, 13469.
16. Kim, J.; Wang, H.-C.; Kumar, J.; Tripathy, S. K. Chem Mater 1999, 11, 2250.
17. Major, J. S.; Blanchard, G. J. Langmuir 2001, 17, 1163.
18. Katz, H. E. Chem Mater 1994, 6, 2227.
19. Krass, H.; Papastavrou, G.; Kurth, D. G. Chem Mater 2003, 15, 196.
20. Lu, Q.; Luo, Y.; Li, L.; Liu, M. Langmuir 2003, 19, 285.
21. Sarathy, K. V.; Thomas, P. V.; Kulkarni, G. U.; Rao, C. N. R. J Phys Chem B 1999, 103, 399.
22. Lee, D.; Rubner, M. F.; Cohen, R. E. Chem Mater 2005, 17, 1099.
23. Zhao, W.; Zheng, B.; Haynie, D. T. Langmuir 2006, 22, 6668.
24. Zhang, L.; Li, B.; Haynie, D. T. Biotechnol Prog 2006, 22, 126.
25. Haynie, D. T.; Balkundi, S.; Chakravarthula, K.; Palath, N.; Dave K. Langmuir 2004, 20, 4540.
26. Boulmedias, F.; Ball, V.; Schwinte, P.; Frisch, B.; Voegel, J.-C. Langmuir 2003, 16, 440.
27. Müller, M. Biomacromolecules 2001, 2, 262.
28. Cheng, Y.; Corn, R. M. J Phys Chem B 1999, 103, 8726.
29. Kim, D. H.; Hernamandez-Lopez, J. L.; Liu, J.; Mihov, G.; Zhi, L.; Bauer, R. E.; Grebel-Köhler, D.; Klapper, M.; Weil, T.; Müllen, K.; Mittler, S.; Knoll, W. Macromol Chem Phys 2005, 206, 52.
30. Hodak, J.; Etchenique, R.; Calvo, E. J.; Singhai, K.; Bartlett, P. N. Langmuir 1997, 13, 2708.
31. Calvo, E. J.; Wolosiuk, A. J Am Chem Soc 2002, 124, 8490.
32. Calvo, E. J.; Etchenique, R.; Pietrasanta, L.; Wolosiuk, A.; Danilowicz, C. Anal Chem 2001, 73, 1161.
33. Beissenhirtz, M. K.; Scheller, F. W.; Stocklein, W. F. M.; Kurth, D. G.; Mohwald, H. L. F. Angew Chem Int Ed 2004, 43, 4357.
34. Beissenhirtz, M. K.; Kafka, J.; Schaefer, D.; Wolny, M.; Lisdat, F. Electroanalysis 2005, 17, 1931.
35. Watanabe, S.; Regan, S. L. J Am Chem Soc 1994, 118, 8855.
36. Zhang, H.; Grim, P. C. M.; Liu, D.; Vosch, T.; De Feyter, S.; Wiesler, U.-M.; Berresheim, A. J.; Müllen, K.; Van Haesendonck, C.; Vandamme, N.; De Schryver, F. C. Langmuir 2002, 18, 1801.
37. Drake, S. K.; Lee, K. L.; Falke, J. J. Biochemistry 1996, 35, 6697.
38. Gagne, S. M.; Li, M. X.; Sykes, B. D. Biochemistry 1997, 36, 4386.
39. Ozawa, T.; Fukuda, M.; Nara, M.; Nakamura, A.; Komine, Y.; Kohama, K.; Umezawa, Y. Biochemistry 2000, 39, 14495.
40. Sharma, Y.; Rao, C. M.; Narasu, M. L.; Rao, S. C.; Somasundaram, T.; Gopalakrishna, A.; Balasubramanian, D. J Biol Chem 1989, 264, 12794.
41. Chen, X.; Zhou, Y.-X.; Xu, Y.-M. Chin Acta Biophys Sinica 1996, 12, 389.
42. Yang, J. L.; Li, H. J.; Yan, H. T. J Chin Rare Earth Soc 1992, 10, 86.
43. Qutierrez, E.; Miller, T. C.; Gonzalez-Redondo, J. R.; Holcombe, J. A. Environ Sci Technol 1999, 33, 1664.
44. Silverman, D. C.; Kalota, D. J.; Stover, F. S. Corros Sci 1995, 51, 818.
45. Appoh, F. E.; Kraatz, H.-B. J Phys Chem C 2007, 111, 4235.
46. Appoh, F. E.; Thomas, D. S.; Kraatz, H.-B. Macromolecules 2005, 38, 7562.
47. Appoh, F. E.; Long, Y.; Kraatz, H.-B. Langmuir 2006, 22, 10515.
48. Legendziewicz, J.; Huskowska, E.; Kozlowski, H.; Jezowska-Trzebiatowska, B. Inorg Nucl Chem Lett 1979, 15, 349.
49. Prados, R.; Stadtherr, L. G.; Donato, J. H.; Martin, R. B. J Inorg Nucl Chem 1974, 36, 689.
50. Dijksma, M.; Boukamp, B. A.; Kamp, B.; van Bennekom, W. P. Langmuir 2002, 18, 3105.
51. Cecchet, F.; Rudolf, P.; Rapino, S.; Margotti, M.; Paolucci, F.; Baggerman, J.; Brouwer, A. M.; Kay, E. R.; Wong, J. K. Y.; Leigh, D. A. J Phys Chem B 2004, 108, 15192.
52. Mendes, R. K.; Freire, R. S.; Fonseca, C. P.; Neves, S.; Kubota, L. T. J Braz Chem Soc 2004, 849.
53. Zugle, R.; Kambo-Dorsa, J.; Gadzekpo, V. P. Y. Talanta 2003, 61, 837.
54. Takehara, K.; Ide, Y.; Aihara, M.; Obunchi, E. Bioelectrochem Bioenergetics 1992, 29, 103.
55. Takehara, K.; Ide, Y.; Aihara, M. Bioelectrochem Bioenergetics 1992, 29, 113.
56. Takehara, K.; Aihara, M.; Ueda, N. Electroanalysis 1994, 6, 1083.
57. Li, J.; Lang, K. S.; Scoles, G.; Ulman, A. Langmuir 1995, 11, 4418.
58. Wang, R.; Schlenoff, J. B. Macromolecules 1998, 31, 494.
59. Uosaki, K.; Sato, Y.; Kita, H. Langmuir 1991, 7, 1510.
60. Rowe, G. K.; Creager, S. E. Langmuir 1991, 7, 2307.
61. Lojou, E.; Bianco, P. J. Electroanal Chem 2003, 557 37.
62. Li, Z.; Hu, N. J. Electroanal Chem 2003, 558, 155.
63. Shen, L.; Hu, N. Biomacromolecules 2005, 6, 1475.
64. Shen, L.; Hu, N. Biochim Biophys Acta 2004, 1608, 23.
65. Sidorenko, A.; Zhai, X. W.; Pelesshanko, S.; Greco, A.; Shevchenko, V. V.; Tsukruk, V. V. Langmuir 2001, 17, 5924.
66. Tsukruk, V. V.; Rinderspacher, F.; Bliznuk, V. N. Langmuir 1997, 13, 2171.
67. Xiao, Z.; Cai, C.; Mayeux, A.; Milenkovic, A. Langmuir 2002, 18, 7728.
68. Blasini, D. R.; Flores-Torres, S.; Smilgies, D. M.; Abruña, H. D. Langmuir 2006, 22, 2082.

69. Tsukruk, V. Adv Mater 1998, 10, 253.
70. Ballauff, M. Topics in Current Chemistry. In Dendrimers III; Vögtle, F., Ed., Springer-Verlag: Heidelberg, 2001, Vol. 212; p 177.
71. Kosal, M. E.; Chou, J.-H.; Suslick, K. S. J Porphyrins Phthalocyanines 2002, 6, 377.
72. Matsuzaki, T.; Iitaka, Y. Acta Crystallogr B: Struct Sci 1972, 28, 1977.
73. Karipides, A.; Reed, A. T. Acta Crystallogr Sect B: Struct Sci 1980, 36, 1377.
74. Fitzgerald, L. J.; Gerkin, R. E. Acta Crystallogr C: Crystallogr Struct Commun 1994, 50, 185.
75. Schuckmann, W.; Fuess, H.; Bats, J. W. Acta Crystallogr B: Struct Sci 1978, 34, 3754.
76. Meehan, E. J. J.; Einspahr, H.; Bugg, C. E. Acta Crystallogr B: Struct Sci 1979, 35, 828.
77. Einspahr, H.; Bugg, C. E. Acta Crystallogr B: Struct Sci 1979, 35, 316.
78. Platers, M. J.; Howie, R. A.; Roberts, A. J. Chem Commun 1997, 893.
79. Appoh, F. E.; Sutherland, T. C.; Kraatz, H.-B. J Organomet Chem 2005, 690, 1209.
80. Appoh, F. E. PhD Thesis, University of Saskatchewan, Saskatoon, SK; 2006.
81. Abbruzzeti, S.; Viappiani, C.; Small, J. R.; Libertini, L. J.; Small, E. W. Biophys J 2000, 79, 2714.
82. Wanunu, M.; Vaskevich, A.; Rubinstein, I. J Am Chem Soc 2004, 126, 5569.
83. Lingenfelder, M. A.; Spillmann, H.; Dmitriev, A.; Stepanow, S.; Lin, N.; Barth, J. V.; Kern, K. Chem Eur J 2004, 10, 1913.
84. Clair, S.; Pons, S.; Brune, H.; Kern, K.; Barth, J. V. Angew Chem Int Ed 2005, 44, 7294.
85. Schlenoff, J. B.; Ly, H.; Li, M. J Am Chem Soc 1998, 120, 7626.
86. Schlenoff, J. B.; Laurent, D.; Ly, H.; Stepp, J. Chem Eng Technol 1998, 21, 757.
87. Lauurent, D.; Schlenoff, J. B. Langmuir 1997, 13, 1552.
88. Uosaki, K.; Kondo, T.; Okamura, M.; Song, W. Faraday Disscuss 2002, 121, 373.
89. Song, W.; Okamura, M.; Kondo, T.; Uosaki, K. Phys Chem Chem Phys 2003, 5, 5279.
90. Song, W.; Okamura, M.; Kondo, T.; Uosaki, K. J Electroanal Chem 2003, 385, 554.
91. Mark, S. S.; Sandhyarani, N.; Zhu, C.; Campagnolo, C.; Batt, C. A. Langmuir 2004, 20, 6808.
92. Bain, C.; Whitesides, G. M. J Phys Chem B 1989, 93, 1670.
93. Douglas, B.; McDaniel, D. H.; Alexander, J. J. Concepts and Models of Inorganic Chemistry; Wiley: Canada, Toronto, 1983.
94. Moser, C. C.; Keske, J. M.; Warncke, K.; Farid, R. S.; Dutton, P. I. Nature 1992, 355, 796.